DUAL CATALYSIS

Merging photoredox with nickel catalysis: Coupling of α-carboxyl sp^3-carbons with aryl halides

Zhiwei Zuo, Derek T. Ahneman, Lingling Chu, Jack A. Terrett, Abigail G. Doyle,* David W. C. MacMillan*

Over the past 40 years, transition metal catalysis has enabled bond formation between aryl and olefinic (sp^2) carbons in a selective and predictable manner with high functional group tolerance. Couplings involving alkyl (sp^3) carbons have proven more challenging. Here, we demonstrate that the synergistic combination of photoredox catalysis and nickel catalysis provides an alternative cross-coupling paradigm, in which simple and readily available organic molecules can be systematically used as coupling partners. By using this photoredox-metal catalysis approach, we have achieved a direct decarboxylative sp^3–sp^2 cross-coupling of amino acids, as well as α-O– or phenyl-substituted carboxylic acids, with aryl halides. Moreover, this mode of catalysis can be applied to direct cross-coupling of C_{sp^3}–H in dimethylaniline with aryl halides via C–H functionalization.

Visible light photoredox catalysis has emerged in recent years as a powerful technique in organic synthesis. This class of catalysis makes use of transition metal polypyridyl complexes that, upon excitation by visible light, engage in single-electron transfer (SET) with common functional groups, activating organic molecules toward a diverse array of valuable transformations (*1*–*5*). Much of the utility of photoredox catalysis hinges on its capacity to generate nontraditional sites of reactivity on common substrates via low-barrier, open-shell processes, thereby fostering the use of abundant and inexpensive starting materials.

Over the past century, transition metal-catalyzed cross-coupling reactions have evolved to be among the most used C–C and C–heteroatom bond-forming reactions in chemical synthesis. In particular, nickel catalysis has provided numerous avenues to forge carbon–carbon bonds via a variety of well-known coupling protocols (Negishi, Suzuki-Miyaura, Stille, Kumada, and Hiyama couplings, among others) (*6*, *7*). The broad functional group tolerance of these reactions enables a highly modular building block approach to molecule construction. Organometallic cross-coupling methods are traditionally predicated on the use of aryl or vinyl boronic acids, zinc halides, stannanes, or Grignard fragments that undergo addition to a corresponding aryl or vinyl halide partner.

We recently questioned whether visible-light photoredox and nickel transition metal catalysis might be successfully combined to create a dual catalysis platform for modular C–C bond formation (Fig. 1) (*8*–*14*). Through a synergistic merger of these two activation modes, we hoped to deliver a mechanism by which feedstock chemicals that contain common yet nontraditional leaving groups (C_{sp^3}–CO_2H or C_{sp^3}–H bonds) could serve as useful coupling partners. Among many advantages, this multicatalysis strategy would enable a modular approach to sp^3–sp^2 or sp^3–sp^3 bond formations that is not currently possible by using either photoredox or transition metal catalysis alone. We sought to develop a general method that would exploit naturally abundant, inexpensive, and orthogonal functional handles (e.g., C–CO_2H, C–H with C–Br, or C–I).

We proposed that two interwoven catalytic cycles might be engineered to simultaneously generate (i) an organometallic nickel(II) species via the oxidative addition of a Ni(0) catalyst to an aryl (Ar), alkenyl, or alkyl halide coupling partner and (ii) a carbon-centered radical generated through a photomediated oxidation event (Fig. 2). Given that organic radicals are known to rapidly combine with Ni(II) complexes (*15*, *16*), we hoped that this dual catalysis mechanism would successfully converge in the form of Ni(III)(Ar)(alkyl) that, upon reductive elimination, would deliver our desired C–C fragment coupling product. One of our laboratories has demonstrated that photoredox catalysis affords access to α-amino radicals by two distinct methods: via decarboxylation of a carboxylic acid or by an oxidation, deprotonation sequence with *N*-aryl or trialkyl amines (*17*, *18*). The other laboratory has explored Ni-catalyzed cross-coupling reactions with iminium ions that proceed via a putative α-aminonickel intermediate (*19*–*21*). Given our respective research areas, we sought to jointly explore the capacity of a nickel (II) aryl species to intercept a photoredox-generated α-amino radical, thereby setting the stage for the fragment coupling. We recognized that the sum of these two catalytic processes could potentially overcome a series of limitations that exist for each of these catalysis methods in their own right.

A detailed description of our proposed mechanistic cycle for the decarboxylative coupling is outlined in Fig. 2. We presumed that initial irradiation of heteroleptic iridium(III) photocatalyst $Ir[dF(CF_3)ppy]_2(dtbbpy)PF_6$ [$dF(CF_3)ppy$ = 2-(2,4-difluorophenyl)-5-(trifluoromethyl)pyridine, dtbbpy = 4,4′-di-*tert*-butyl-2,2′-bipyridine] (**1**) would produce the long-lived photoexcited $*Ir^{III}$ state **2** (exposure time τ = 2.3 μs) (*22*). Deprotonation of the α-amino acid substrate **3** with base and oxidation by the excited-state $*Ir^{III}$ complex {$E_{1/2}^{red}$ [$*Ir^{III}/Ir^{II}$] = +1.21 V versus saturated calomel electrode (SCE) in CH_3CN} (*22*) via a SET event would then generate a carboxyl radical, which upon rapid loss of CO_2 would deliver

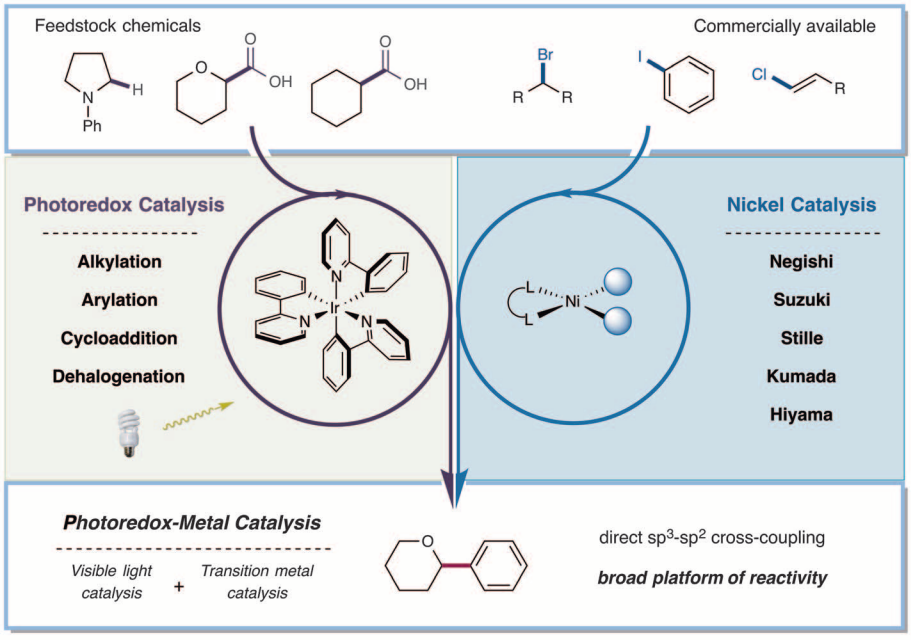

Fig. 1. The merger of photoredox and nickel catalysis yields access to direct sp^3-sp^2 cross-coupling. R, alkyl group.

Merck Center for Catalysis at Princeton University, Princeton, NJ 08544, USA.
*Corresponding author. E-mail: agdoyle@princeton.edu (A.G.D.); dmacmill@princeton.edu (D.W.C.M.)

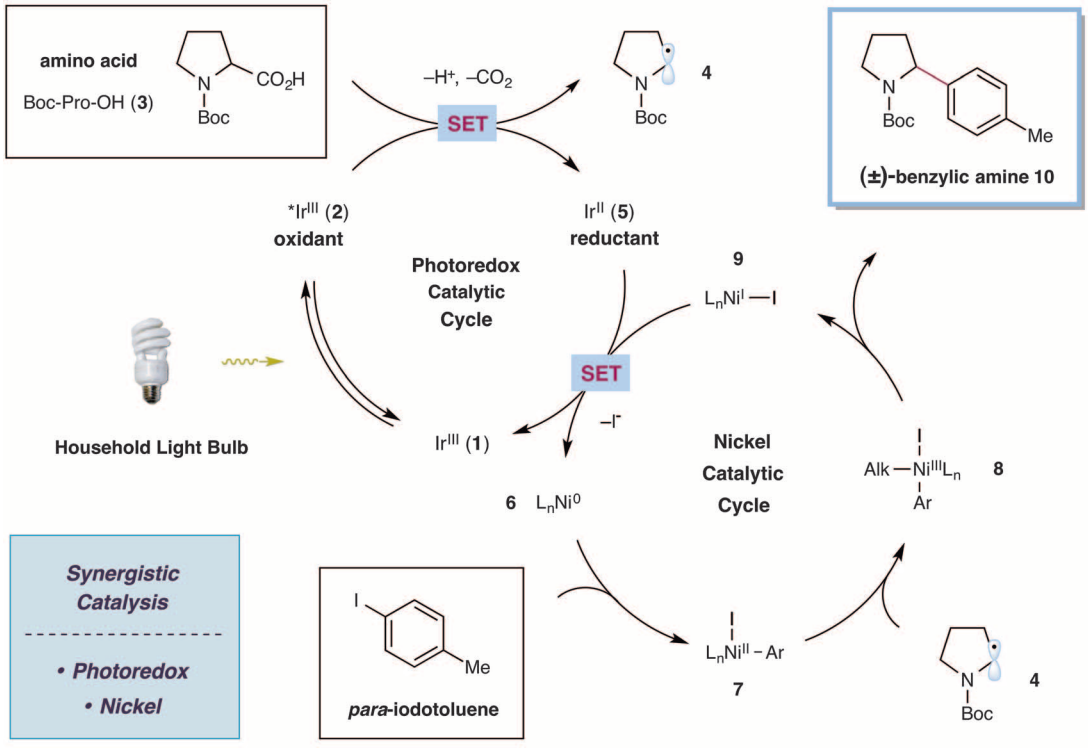

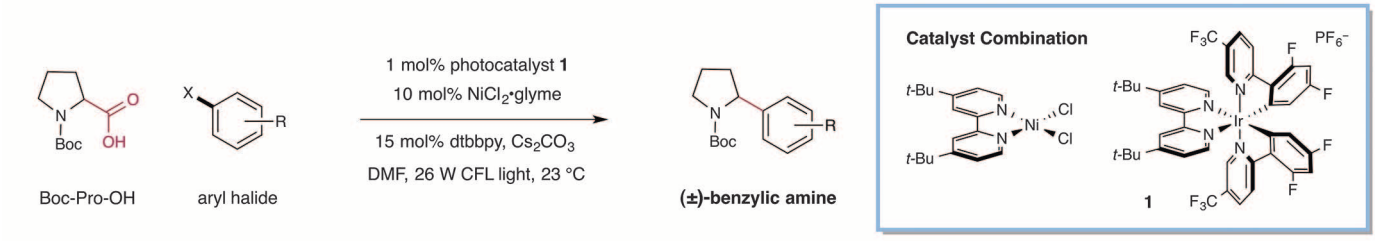

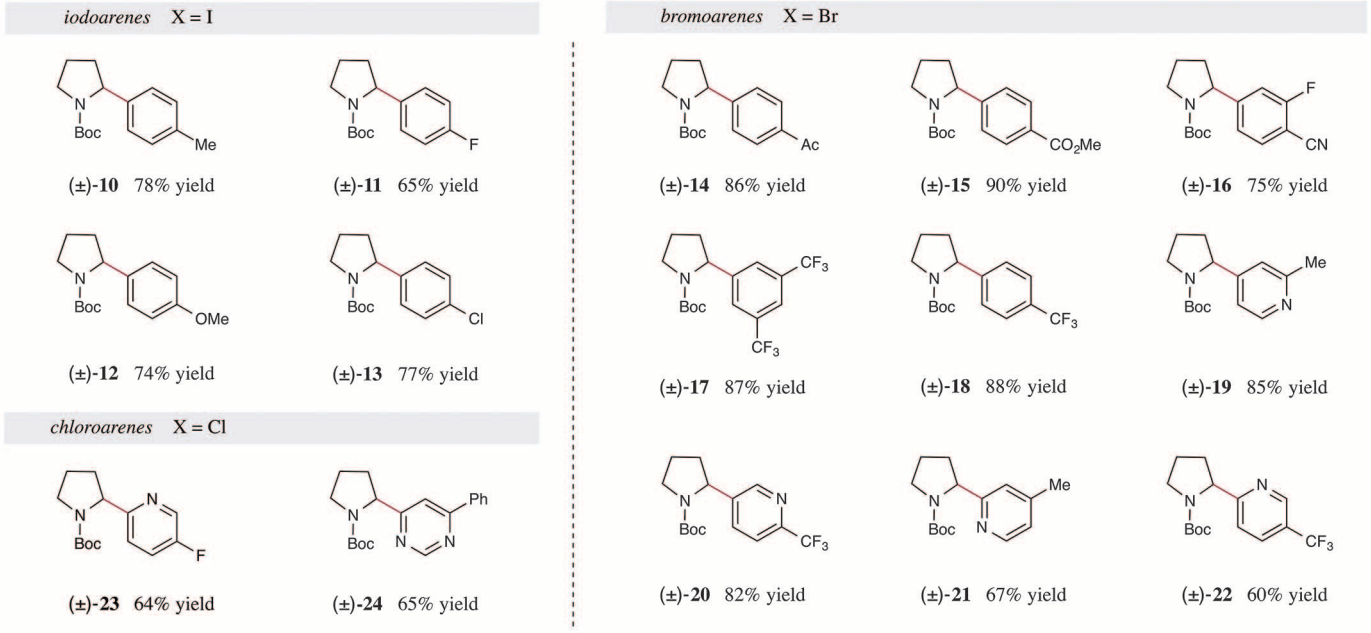

Fig. 2. Proposed mechanistic pathway of photoredox-nickel-catalyzed decarboxylative arylation. Me, methyl group; L, ligand; Alk, alkyl group.

Fig. 3. Photoredox-nickel catalyzed decarboxylative cross-coupling: aryl halide scope. CFL, compact fluorescent light; Bu, butyl group; Ac, acetyl group.

the α-amino radical **4** and the corresponding Ir^{II} species **5**. Given the established oxidation potential of prototypical amino acid carboxylate salts, we expected this process to be thermodynamically favorable [*tert*-butyl carbamoyl (Boc)–Pro-OCs, $E_{1/2}^{red}$ = +0.95 V versus SCE in CH_3CN) (*17*). Concurrently with this photoredox cycle, we hoped that oxidative addition of the Ni(0) species **6** into an aryl halide would produce the Ni(II) intermediate **7**. We anticipated that this Ni(II)-aryl species would rapidly intercept the α-amino radical **4**, forming the organometallic Ni(III) adduct **8**. Subsequent reductive elimination would forge the requisite C–C bond while delivering the desired α-amino arylation product **10** and expelling the Ni(I) intermediate **9**. Last, SET between the Ir^{II} species **5** and the Ni complex **9** would accomplish the exergonic reduction of Ni(I) to Ni(0) {on the basis of the established two-electron reduction potential of Ni(II) to Ni(0), we presume that reduction of Ni(I) to Ni(0) should be thermodynamically favorable, $E_{1/2}^{red}$ [Ni^{II}/Ni^{0}] = –1.2 V versus SCE in *N*,*N*´-dimethylformamide (DMF)} by the Ir^{II} species **5** {$E_{1/2}^{red}$ [Ir^{III}/Ir^{II}] = –1.37 V versus SCE in CH_3CN} (*22*, *23*), thereby completing both the photoredox and the nickel catalytic cycles simultaneously.

With this mechanistic hypothesis in hand, we first examined the proposed coupling by using *N*-Boc proline, *para*-iodotoluene, and a wide range of photoredox and ligated nickel catalysts. To our delight, we found that the combination of Ir[dF(CF_3)ppy]$_2$(dtbbpy)PF_6 and $NiCl_2$•glyme (glycol ether), dtbbpy, in the presence of 1.5 equivalents of Cs_2CO_3 base and white light from a 26-W compact fluorescent bulb, achieved the desired fragment coupling in 78% yield. During our optimization studies, we found that use of a bench-stable Ni(II) source, such as $NiCl_2$•glyme, was sufficient to generate the arylation product with comparable efficiency to a Ni(0) source. We attribute this result to in situ photocatalytic reduction of Ni(II) to Ni(0) via two discrete SET events, with excess amino acid likely serving as the sacrificial reductant to access the active Ni catalyst {$E_{1/2}^{red}$ [Ni^{II}/Ni^{0}] = –1.2 V versus SCE in DMF} (*23*). We believe that it is unlikely that the Ni(II)(Ar)X intermediate **7** undergoes a SET event to form Ni(I)Ar, given the poorly matched reduction potentials of the species involved {compare with $E_{1/2}^{red}$ [Ni^{II}ArX/Ni^{I}Ar] = –1.7 V versus SCE in CH_3CN and $E_{1/2}^{red}$ [Ir^{III}/Ir^{II}] = –1.37 V versus SCE in CH_3CN} (*22*, *24*). However, we recognize that an alternative pathway could be operable wherein the oxidative addition step occurs from the Ni(I) complex to form a Ni(III) aryl halide adduct. In this pathway, photocatalyst-mediated reduction of the aryl-Ni(III) salt to the corresponding Ni(II) species followed by the α-amino radical addition step would then form the same productive Ni(III) adduct **8**, as shown in Fig. 2. Given that (i) Ni(0) complexes undergo oxidative addition more readily than Ni(I) complexes with aryl halides (*25*) and (ii) Ni(II) complexes are believed to rapidly engage with sp^3 carbon-centered radicals to form Ni(III) species (enabling sp^3–sp^2 and sp^3–sp^3 C–C bond formations) (*15*, *16*), we favor the dual-catalysis mechanism outlined in Fig. 2.

Having established the optimal conditions for this photoredox-nickel decarboxylative arylation, we focused our attention on the scope of the aryl halide fragment. As shown in Fig. 3, a wide range of aryl iodides are amenable to this dual-catalysis strategy, including both electron-rich and electron-deficient arenes (**10** to **13**, *65*

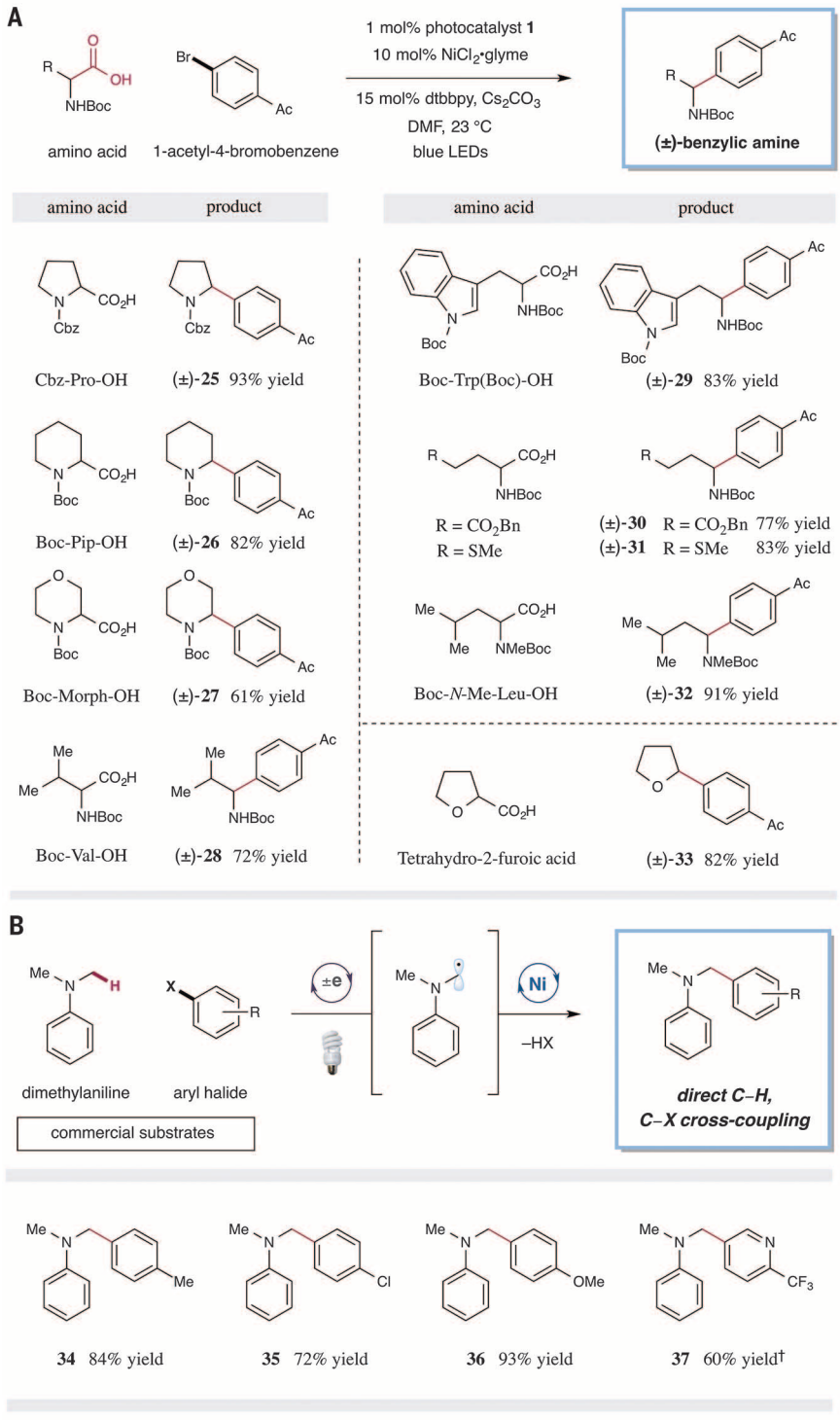

Fig. 4. Amino acid coupling partners and C_{sp^3}–H, C–X cross-coupling. (**A**) Evaluation of the amino acid coupling partner in the decarboxylative-arylation protocol. Ac, acetyl group; LED, light-emitting diode. (**B**) The direct C_{sp^3}–H, C–X cross-coupling via photoredox-nickel catalysis. All yields listed in Figs. 3 and 4 are isolated yields. Reaction conditions for (A) are the same as in Fig. 3. Reaction conditions for (B) are as follows: photocatalyst **1** [1 mole % (mol %)]; $NiCl_2$·glyme (10 mol %), dtbbpy (15 mol %), KOH (3 equiv.), DMF, 23°C, 26-W light. *Iodoarenes used as aryl halide, X = I. †Bromoarene used, X = Br.

to 78% yield). Many aryl bromides function effectively as well, including those that contain functional groups as diverse as ketones, esters, nitriles, trifluoromethyl groups, and fluorides (**14** to **18**, 75 to 90% yield). Heteroaromatics, in the form of differentially substituted bromopyridines, are also efficient coupling partners (**19** to **22**, 60 to 85% yield). Moreover, aryl chlorides are competent substrates if the arenes, such as pyridines and pyrimidines, are electron-deficient (**23** and **24**, 64 and 65% yield). Only products **15** and **19** in Fig. 3 would be accessible by using our previously reported photoredox arylation strategy. Moreover, we are unaware of the general use of C_{sp^3}-bearing carboxylic acids as reaction substrates in transition metal catalysis, an illustration of the tremendous scope expansion that is attainable by using this dual catalysis technology. These reactions are typically complete in 72 hours at larger scale and 48 hours on smaller scale (see supplementary text).

Next, we investigated the nature of the carboxylic acid coupling partner, as highlighted in Fig. 4A. A wide variety of α-amino acids function effectively in this protocol, including various *N*-Boc and *N*-benzyl carbamoyl (*N*-Cbz) protected heterocycles (**25** to **27**, 61 to 93% yield). Acyclic α-amino acids, containing indole, ester, and thioether functionalities, are also readily tolerated (**28** to **32**, 72 to 91% yield). α-oxycarboxylic acids can function as proficient coupling partners, producing α-arylated ethers in high yield over a single step (**33**, 82% yield). Moreover, we have also found that various phenyl acetic acid substrates function in this coupling protocol with high efficiency (>78% yield, see supplementary text).

To further demonstrate the utility of this dual-catalysis strategy, we sought to demonstrate the direct functionalization of C_{sp^3}–H bonds with coupling partners derived from aryl or alkyl halides. Given that our decarboxylation-arylation mechanism involves the rapid addition of an α-amino radical to a Ni(II) salt, we sought to generate an analogous α-nitrogen carbon–centered radical via a photoredox-driven *N*-phenyl (*N*-Ph) oxidation, α-C–H deprotonation sequence using aniline-based substrates (*18*). We presumed that this photomediated *N*-Ph oxidation mechanism would provide an alternative pathway to the open-shell carbon intermediate (corresponding to **4**, Fig. 2) and should similarly intercept the putative Ni(II) intermediate **8**. Assuming that the remaining dual-catalysis mechanism would be analogous to that shown in Fig. 2, we expected that a range of direct C_{sp^3}–H functionalization protocols should be possible. Indeed, we were able to demonstrate that dimethylaniline undergoes α-amine coupling with a variety of aryl halides in the presence of $Ir[dF(CF_3)ppy]_2(dtbbpy)PF_6$ and $NiCl_2$•glyme (Fig. 4B). Electron-deficient and electron-rich iodoarenes give moderate to high yields (**34** to **36**, 72 to 93% yield). Moreover, aryl bromides are competent coupling partners, enabling the installation of medicinally important heterocyclic motifs (**37**, 60% yield). Last, control experiments have revealed that the combination of light, photoredox catalyst **1**, and the $NiCl_2$•dtbbpy complex is essential for product formation in all examples listed in Figs. 3 and 4. This reaction represents a powerful foray into direct C–H activation using orthogonal cross-coupling reactivity.

REFERENCES AND NOTES

1. D. A. Nicewicz, D. W. C. MacMillan, *Science* **322**, 77–80 (2008).
2. M. A. Ischay, M. E. Anzovino, J. Du, T. P. Yoon, *J. Am. Chem. Soc.* **130**, 12886–12887 (2008).
3. J. M. R. Narayanam, J. W. Tucker, C. R. J. Stephenson, *J. Am. Chem. Soc.* **131**, 8756–8757 (2009).
4. D. S. Hamilton, D. A. Nicewicz, *J. Am. Chem. Soc.* **134**, 18577–18580 (2012).
5. M. T. Pirnot, D. A. Rankic, D. B. C. Martin, D. W. C. MacMillan, *Science* **339**, 1593–1596 (2013).
6. M. R. Netherton, G. C. Fu, *Adv. Synth. Catal.* **346**, 1525–1532 (2004).
7. A. Rudolph, M. Lautens, *Angew. Chem. Int. Ed.* **48**, 2656–2670 (2009).
8. The successful merger of photoredox and transition metal catalysis has been demonstrated for the specific installation of unique functionality (e.g., CF_3) (*9*–*14*).
9. M. Osawa, H. Nagai, M. Akita, *Dalton Trans.* **2007**, 827–829 (2007).
10. D. Kalyani, K. B. McMurtrey, S. R. Neufeldt, M. S. Sanford, *J. Am. Chem. Soc.* **133**, 18566–18569 (2011).
11. Y. Ye, M. S. Sanford, *J. Am. Chem. Soc.* **134**, 9034–9037 (2012).
12. M. Rueping *et al.*, *Chemistry* **18**, 5170–5174 (2012).
13. B. Sahoo, M. N. Hopkinson, F. Glorius, *J. Am. Chem. Soc.* **135**, 5505–5508 (2013).
14. X. Z. Shu, M. Zhang, Y. He, H. Frei, F. D. Toste, *J. Am. Chem. Soc.* **136**, 5844–5847 (2014).
15. S. Biswas, D. J. Weix, *J. Am. Chem. Soc.* **135**, 16192–16197 (2013).
16. S. L. Zultanski, G. C. Fu, *J. Am. Chem. Soc.* **135**, 624–627 (2013).
17. Z. Zuo, D. W. C. MacMillan, *J. Am. Chem. Soc.* **136**, 5257–5260 (2014).
18. A. McNally, C. K. Prier, D. W. C. MacMillan, *Science* **334**, 1114–1117 (2011).
19. T. J. A. Graham, J. D. Shields, A. G. Doyle, *Chem. Sci.* **2**, 980 (2011).
20. K. T. Sylvester, K. Wu, A. G. Doyle, *J. Am. Chem. Soc.* **134**, 16967–16970 (2012).
21. J. D. Shields, D. T. Ahneman, T. J. A. Graham, A. G. Doyle, *Org. Lett.* **16**, 142–145 (2014).
22. M. S. Lowry *et al.*, *Chem. Mater.* **17**, 5712–5719 (2005).
23. M. Durandetti, M. Devaud, J. Perichon, *New J. Chem.* **20**, 659 (1996).
24. Y. H. Budnikova, J. Perichon, D. G. Yakhvarov, Y. M. Kargin, O. G. Sinyashin, *J. Organomet. Chem.* **630**, 185–192 (2001).
25. C. Amatore, A. Jutand, *Organometallics* **7**, 2203–2214 (1988).

ACKNOWLEDGMENTS

The authors are grateful for financial support provided by the NIH General Medical Sciences (grants NIHGMS R01 GM103558-01 and R01 GM100985-01) and gifts from Merck, Amgen, Eli Lilly, and Roche. Z.Z. and L.C. are grateful for postdoctoral fellowships from the Shanghai Institute of Organic Chemistry. The authors thank G. Molander and co-workers for graciously offering to concurrently publish a related study that was submitted slightly ahead of our own.

SUPPLEMENTARY MATERIALS

www.sciencemag.org/content/345/6195/437/suppl/DC1
Material and Methods
Supplementary Text
Tables S1 and S2
Data
References (*26*–*34*)

1 May 2014; accepted 27 May 2014
Published online 5 June 2014;
10.1126/science.1255525

EXOPLANET DETECTION

Stellar activity masquerading as planets in the habitable zone of the M dwarf Gliese 581

Paul Robertson,[1,2]* Suvrath Mahadevan,[1,2,3] Michael Endl,[4] Arpita Roy[1,2,3]

The M dwarf star Gliese 581 is believed to host four planets, including one (GJ 581d) near the habitable zone that could possibly support liquid water on its surface if it is a rocky planet. The detection of another habitable-zone planet—GJ 581g—is disputed, as its significance depends on the eccentricity assumed for d. Analyzing stellar activity using the Hα line, we measure a stellar rotation period of 130 ± 2 days and a correlation for Hα modulation with radial velocity. Correcting for activity greatly diminishes the signal of GJ 581d (to 1.5 standard deviations) while significantly boosting the signals of the other known super-Earth planets. GJ 581d does not exist, but is an artifact of stellar activity which, when incompletely corrected, causes the false detection of planet g.

At a distance of 6.3 parsecs, the M dwarf star Gliese 581 (GJ 581) is believed to host a system of planets discovered using the Doppler radial velocity (RV) technique (*1*–*3*) and a debris disk (*4*). It is considered a local analog to compact M dwarf planetary systems found by the Kepler spacecraft (*5*, *6*).

Although the periods and orbital parameters of the inner planets b (P = 5.36 days) and c (P = 12.91 days) are unchanged since their initial discovery (*1*, *2*), the period of planet d was revised from 82 to 66 days (*2*, *3*) upon the discovery of a fourth planet e (P = 3.15 days). Using a combination of data from the High Accuracy Radial Velocity Planet Searcher (HARPS) spectrograph and the High Resolution Echelle Spectrometer (HIRES), planets f (P = 433 days) and g (P = 36.5 days) were reported (*7*), and their existence promptly questioned (*8*) using additional data from HARPS. Although the reported

Science

Merging photoredox with nickel catalysis: Coupling of α-carboxyl sp^3-carbons with aryl halides

Zhiwei Zuo, Derek T. Ahneman, Lingling Chu, Jack A. Terrett, Abigail G. Doyle and David W. C. MacMillan

Science **345** (6195), 437-440.
DOI: 10.1126/science.1255525originally published online June 5, 2014

A bright outlook for carbon coupling

In contemporary organic chemistry, it is straightforward to forge bonds between unsaturated carbons (i.e., carbons already engaged in double bonds) using cross-coupling catalysis. The protocol runs into some trouble, however, if one or both starting carbon centers are saturated (purely single-bonded). Tellis *et al.* and Zuo *et al.* independently found that combining a second, light-activated catalyst with a nickel cross-coupling catalyst could achieve selective coupling of saturated and unsaturated reagents (see the Perspective by Lloyd-Jones and Ball). Their methods rely on single-electron transfer from the light-activated catalyst to the saturated carbon, thereby enhancing its reactivity more effectively than the twoelectron mechanisms prevailing in traditional protocols.

Science, this issue p. 433, p. 437; see also p. 381